Nonlinear Systems and Complexity
Series Editor: Albert C. J. Luo

Jian-Qiao Sun · Albert C. J. Luo
Editors

Global Analysis of Nonlinear Dynamics

Springer

Global Analysis of Nonlinear Dynamics

Jian-Qiao Sun • Albert C.J. Luo
Editors

Global Analysis of Nonlinear Dynamics

Springer

Editors
Jian-Qiao Sun
School of Engineering
University of California
Merced, CA, USA

Albert C.J. Luo
School of Engineering
Mechanical and Industrial Engineering
Southern Illinois University
Edwardsville, IL, USA

ISBN 978-1-4614-3127-5 e-ISBN 978-1-4614-3128-2
DOI 10.1007/978-1-4614-3128-2
Springer New York Dordrecht Heidelberg London

Library of Congress Control Number: 2012936649

Printed on acid-free paper

Springer is part of Springer Science+Business Media (www.springer.com)

On behalf of his graduate students, visiting scholars, colleagues and friends all over the world, we dedicate this book to Professor Chien-Su Hsu on the occasion of his 90th birthday in May 2012.

J.Q. Sun and A.C.J. Luo

Professor C.S. Hsu was born in Suzhou, China, on May 27, 1922, and is a US citizen. He received his MS and PhD degrees in engineering mechanics from Stanford University under the supervision of Professor J.N. Goodier in 1948 and 1950, respectively. From 1951 to 1955, he was an engineer at IBM. He started his academic career first at the University of Toledo (1955–1958) and moved to U.C. Berkeley in 1958 where he remained for 33 years until his retirement in 1991.

Professor Hsu was a recipient of John Simon Guggenheim Fellowship in 1964–1965, held a Miller Research Professorship of UC Berkeley in 1973–1974, became a Fellow of ASME in 1977, a Fellow of American Academy of Mechanics in 1980, an elected member of National Academy of Engineering in 1988, an elected member of Academia Sinica of Republic of China in 1990, a recipient of the Alexander von Humbolt Senior US Scientist Award in 1986, the ASME N.O. Myklestad Award in 1995, and the ASME J.P. Den Hartog Award in 2011. He served as the Technical Editor of *ASME Journal of Applied Mechanics* in 1976–1982, and in editorial capacities for ten prestigious journals representing the fields of nonlinear mechanics and dynamics including *Solid Mechanics Archives*, *Acta Mechanica*, *Journal of Applied Mathematics and Mechanics*, *International Journal of Non-linear Mechanics*, and *Bifurcation and Chaos in Applied Science and Engineering*.

Foreword

It is an honor to contribute the Foreword to this book that celebrates the 90th birthday of Professor C.S. Hsu. Professor Hsu remains a giant in the field of nonlinear dynamics through his remarkable achievements as an educator and as a researcher.

Professor Hsu's distinguished career in mechanics originated with his doctoral research at Stanford University (with J.N. Goodier) and flourished at the University of California at Berkeley where he pursued his academic career. While it is hard to estimate the number of students he taught during his entire career, that number must be measured in the units of thousands. His enormous reach as an educator was powered through a premier sequence of four graduate courses he developed at U.C. Berkeley. These courses, in linear vibration theory, random vibrations, nonlinear oscillations, and elastic stability, provided fertile training for generations of aspiring researchers in our field. For each course, Professor Hsu amassed original research papers, a few text books, and elegant notes. His lectures were, in a word, brilliant. He conveyed his thoughts with uncommon clarity, distilled each topic to its essence, and engaged students in lively discussions both in and outside the classroom. Like many of his former students, I resort to his course notes time and time again, both in the context of my research and for the courses I now offer. He is, without doubt, a magnificent educator who has influenced the trajectory of thousands of very fortunate students.

This book, conceived and edited by Professors Jian-Qiao Sun and Albert C. J. Luo, celebrates Professor Hsu's seminal contributions to nonlinear dynamics through his research in parametrically excited structures, global analysis of nonlinear systems, and cell-to-cell mapping. His contributions have profoundly influenced the thinking of scholars worldwide as evidenced, in part, by the 11 contributions featured in this volume. In particular, Professor Hsu's pioneering research on cell-to-cell mapping is prominently featured herein. At its core, cell-to-cell mapping is as simple as it is elegant, as the best ideas always are. The method begins with discretizing continuous state–space into a finite number of cells and computing the forward map emanating from each cell. This map, often determined numerically, determines the fate of the

flow in state–space and thus the global behavior of the dynamical system. Cell-to-cell mapping is a powerful method that yields attractors and their domains of attraction in a highly organized and efficient manner. Since the early 1980s, Professor Hsu and his collaborators discovered the fundamental mathematical properties of cell-to-cell mapping techniques and advanced these in numerous directions. The major developments are summarized in Professor Hsu's highly regarded treatise, *Cell-to-Cell Mapping—A Method of Global Analysis of Nonlinear Systems*, published in 1987 by Springer-Verlag applied mathematical sciences series. It remains the bible for cell-to-cell mapping.

We invite you to enjoy and share the contributions selected for this volume which celebrate the giant achievements of Professor C.S. Hsu on the occasion of his 90th birthday. And on behalf of his collaborators, his many students, and all of his admirers, we warmly wish him many fine returns of the day!

Ann Arbor, MI, USA Noel Perkins

Preface

This book is dedicated to Dr. C.S. Hsu, emeritus professor of University of California at Berkeley in honor of his 90th birthday in May 2012. In the past 50 years, Professor Hsu has made broad and significant contributions to the theory and practice of nonlinear dynamics. His publications have inspired and influenced many researchers around the world. We have invited a group of active researchers in the area of nonlinear dynamics to contribute chapters to this book. The authors of the chapters present their recent research that has been motivated by the work done by Professor Hsu.

Professor Hsu invented the cell-to-cell mapping method for the global analysis of nonlinear dynamical systems. This method has helped us to better understand the complex behavior of nonlinear dynamical systems including stable and unstable invariant sets, attraction domain, and strange attractors. Chapters 3–6 are devoted to the new developments of the cell mapping method with the help of graph theory and the multiple scale approach. The cell mapping method has also been applied to study control problems. Chapters 1–2 present studies of tuning feedback controls with the help of the cell mapping method, while Chapter 11 is devoted to optimal control problems of nonlinear stochastic systems with the generalized cell mapping method. The generalized cell mapping was extended to the fuzzy dynamical systems in the early 1990s. Chapter 7 presents a bifurcation study of nonlinear dynamical systems with fuzzy parameters or excitations. The set-oriented method represents a significant refinement of the cell mapping method for determining invariant sets and finding zeros of nonlinear vector functions. Chapter 10 presents an excellent study on this topic.

Professor Hsu has also done systematical studies on the Lyapunov stability of continuous structures and the stability of parametric dynamical systems. These studies laid a solid foundation for the subsequent development of the field of nonlinear mechanics and dynamics. Chapter 8 presents a study of stability and responses of nonlinear structures. Chapter 9 presents a comprehensive study of the chaos in parametric nonlinear dynamical systems.

This collection of recent developments in nonlinear dynamical systems brings new and different perspectives and can serve as a good reference to the community of nonlinear dynamics in different disciplines including engineering, applied mathematics, meteorology, life science, computational science, and medicine. It is our intention that this book will stimulate the interests in global analysis of complex and high-dimensional nonlinear dynamical systems, whose global properties are largely unexplored at this time.

Finally, we would like to thank all the chapter contributors and reviewers for their time and effort making this gift to Professor Hsu's 90th birthday under a tight schedule.

Merced, CA, USA Jian-Qiao Sun
Edwardsville, IL, USA Albert C.J. Luo

Contents

1 Global Analysis of Periodic Solutions for Flexible Feedback Systems 1
Michael Borre and Henryk Flashner

2 Cell Mapping Techniques for Tuning Dynamical Systems..... 31
Ángela Castillo and Pedro J. Zufiria

3 Iterative Digraph Cell Mapping Method 51
Wei Xu, Xiaole Yue, and Qun He

4 Crises in Chaotic Systems..... 75
Ling Hong and Jian-Xue Xu

5 Point Mapping under Cell Reference - A Two Scaled Numerical Method for Global Analysis..... 107
Jun Jiang and Jian-Xue Xu

6 Unstable Invariant Sets in Nonlinear Dynamical Systems 139
Hai-Lin Zou and Jian-Xue Xu

7 Fuzzy Cell Mapping..... 161
Jian-Qiao Sun and Ling Hong

8 Stability and Response Bounds for Structures Under Dynamic Loads 175
Raymond H. Plaut

9 Hamiltonian Chaos in Nonlinear Parametric Systems 189
Albert C.J. Luo

10 Multilevel Subdivision Techniques for Scalar Optimization Problems 221
Michael Dellnitz and Oliver Schütze

11 Stochastic Control 253
Jian-Qiao Sun

Index 277

Chapter 1
Global Analysis of Periodic Solutions for Flexible Feedback Systems

Michael Borre and Henryk Flashner

Abstract A method for calculating all periodic solutions and their domains of attraction for flexible systems under nonlinear feedback control is presented. The systems considered consist of mechanical systems with many flexible modes and a relay type controller coupled with a nonlinear control law operating in a feedback configuration. The proposed approach includes three steps. First, limit cycle frequencies and periodic fixed points are computed exactly, using a block diagonal state–space modal representation of the plant dynamics. Then the relay switching surface is chosen as the Poincare mapping surface and is discretized using the cell mapping method. Finally, the region of attraction for each limit cycle is computed using the cell mapping algorithm and employing an error based convergence criterion. An example consisting of a model of a flexible system, a relay with dead-zone and hysteresis, and a nonlinear control law is used to demonstrate the proposed approach.

1.1 Introduction

In many important engineering applications, the objective of mechanical control systems is to generate periodic behavior (limit cycle) of given amplitude and frequency. For example, in the case of spacecraft attitude control systems utilizing thruster actuators, the goal is to generate a periodic motion of given amplitude and frequency, in order to minimize fuel consumption, while meeting spacecraft

M. Borre • H. Flashner (✉)
Department of Aerospace and Mechanical Engineering, University of Southern California, Los Angeles, CA 90089-1453, USA
e-mail: borre@usc.edu; hflashne@usc.edu

J.-Q. Sun and A.C.J. Luo (eds.), *Global Analysis of Nonlinear Dynamics*,
DOI 10.1007/978-1-4614-3128-2_1,

pointing requirements. The control law is often performed using a Schmitt trigger that together with the discontinuous nature of the on–off thruster actuators is modeled as a relay with dead-zone and hysteresis (Agrawal et al. 1997; Bryson 1994; Martin and Bryson 1978; Sidi 2002; Wie 1998).

Analysis of discontinuous control laws of mechanical and aerospace systems has been mainly performed assuming a rigid body. However, in many mechanical systems, strict performance specifications in the form of high bandwidth and the system's weight limitations cause a large number of flexible modes to be within the control system's bandwidth, thus requiring their inclusion in the system model. The presence of many lightly damped modes in the model may lead to a highly complex periodic behavior that requires careful analysis. Understanding the relation between the control law, system flexible dynamics, and periodic motion characteristics, such as amplitude and frequency of periodic motion, are of paramount importance for achieving closed-loop performance specifications.

The class of systems investigated in this chapter consists of a linear mechanical system that includes flexible structural modes, a feedback control law that includes a linear or nonlinear controller, and a discontinuous control law in the form of a relay with dead-zone and hysteresis. Systems of this type can be classified as relay feedback control systems (RFCS). For the spacecraft attitude control application, station-keeping pointing operations require a prescribed limit cycle with specified frequency and amplitude. When the control torques are generated using thrusters, strict performance specifications on the limit cycle amplitude may require including flexible modes in the design model. Flexible modes may alter the frequency and amplitude of the limit cycle and may generate additional stable periodic modes of behavior. Finding the various limit cycles and their domains of attraction are of the utmost importance for understanding the behavior of the closed-loop system and improve performance.

Current solution techniques to solve for the multimodal limit cycle frequencies in RFCS can be grouped into three categories—frequency based, time based, and cell mapping. Frequency-based methods include the describing function method (DFM) (Gelb and Vander Velde 1968) and the more accurate Tsypkin's Method (Tsypkin 1984). The DFM assumes that the response of the system during a limit cycle is a pure sinusoid, whereas Tsypkin's Method allows for more complex limit cycle waveforms, using a truncated Fourier series approximation. Extensions of the Tsypkin method also using the Fourier series expansion are done by Atherton (1976) and Boiko (2009). A limitation to the frequency-based methods is that they provide no information on periodic fixed points of the limit cycle. Also, they provide no information on global stability of the limit cycle, which is especially important when multiple limit cycles are possible for the system.

Time-based methods analyze the relay switching instances using a state–space formulation as demonstrated in Astrom (1995). This allows the determination of a limit cycle fixed point location in state–space coordinates. Also, the waveform solution is exact, and is equivalent to the infinite term Fourier series solution used in Tsypkin's Method. However, like the frequency methods, these methods provide no information on global stability for multiple limit cycles.

In order to determine global stability for multiple limit cycles, the cell mapping method developed by Hsu (Hsu 1980, 1981, 1987; Hsu and Guttalu 1980; Hsu and Kim 1985; Hsu et al. 1982; Kreuzer and Lagemann 1996; Xu et al. 1985) can be used to map the region of attraction about each periodic fixed point. The cell mapping method discretizes the state space into individual cells, with each cell center serving as an initial condition for the mapping process. This method and its extensions were applied to different types of deterministic and stochastic systems. An extension of Hsu's method was proposed by Levitas (Levitas and Weller 1993; Levitas et al. 1994, 1997) where a hypersurface is used as a system constraint to reduce the dimension of the cell space by one, compared to Hsu's method. This leads to a substantial reduction in the total number of cells, especially for higher-order systems.

An alternate approach to finding global domains of attraction for dynamic systems is backward mapping as proposed by Flashner and Guttalu (Flashner and Guttalu 1988; Guttalu and Flashner 1988). This method integrates the system equations backwards in time from an initial set of seed points surrounding a periodic fixed point. The resulting set of points at the end of the backward integration form the domain of attraction, since points within this region will head for the initial fixed point when integrated forward in time. This method, however, cannot be used for the problem at hand due to memory in the system, caused by the hysteresis in the relay. Backward integration would require future knowledge of the switching times, in order for the system trajectories to be the same under both backward and forward integration. Thus, only forward integrating techniques such as Hsu's simple cell mapping (SCM) technique can be used for finding global domains of attraction for periodic systems that contain hysteresis.

A computational approach for accurately computing limit cycles and their regions of attraction (ROA) for mechanical systems with multiple flexible modes is presented in this chapter. The method employs a block-diagonal state–space modal formulation, allowing for a closed form solution of the relay switching constraint equations used in determining limit cycle frequencies and fixed points. The method also presents a modification of the cell mapping method, which significantly reduces memory requirements with increased solution accuracy, so that more flexible modes may be considered in the plant model.

The chapter is organized into four sections as follows. The class of systems under consideration is defined in Sect. 2. Section 3 presents a procedure for accurate computation of limit cycles and fixed points for this class of systems. Section 4 describes a method for determining the domains of attraction of these limit cycles. Finally, in Sect. 5 an illustrative example problem consisting of a model of a flexible spacecraft is presented to demonstrate the method proposed in this study.

1.2 System Definition

Consider the following single-input-single-output (SISO) system shown in Fig. 1.1. The controller is of general form and may be linear such as proportional-integral-derivative (PID) or nonlinear, with system position error as input. The controller

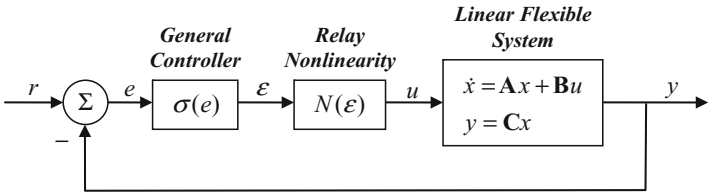

Fig. 1.1 SISO feedback control with relay nonlinearity and flexible modes

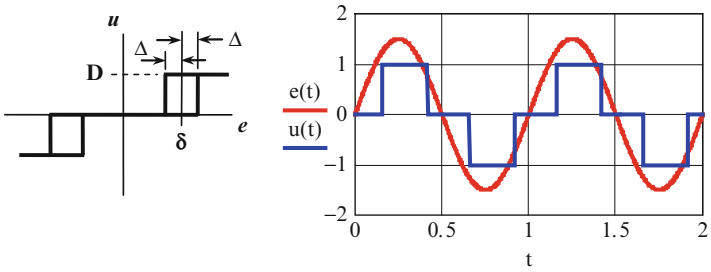

Fig. 1.2 Relay with dead-zone and hysteresis

output provides an input signal to a relay nonlinearity, which in turn provides an on–off fixed magnitude input to the flexible system, which is comprised of a rigid-body mode, and n lightly damped structural modes.

1.2.1 Relay Type

The relay type investigated here is a relay with dead-zone and hysteresis as shown in Fig. 1.2. The relay output u is switched between $-$D,0,+D by the input signal e, as the input magnitude crosses the dead-zone and hysteresis bands $\delta \pm \Delta$ shown in the figure. The magnitude of $u(t)$ within the hysteresis band depends on its immediately preceding value $u(t-)$.

1.2.2 Plant

The modal summation form of the undamped flexible system equations is used as a starting point in formulating the *block-diagonal state matrices*, used in the proposed method. The modal summation form can be developed using the undamped n-degree-of-freedom system of equations given by:

$$\mathbf{M}\ddot{\mathbf{q}}(t) + \mathbf{K}\mathbf{q}(t) = \mathbf{F}(t) \tag{1.1}$$

where $\mathbf{q}$ is an $n \times 1$ vector of physical coordinates, $\mathbf{M}$ and $\mathbf{K}$ are symmetric $n \times n$ mass and stiffness matrices, and $\mathbf{F}$ is an $n \times 1$ force vector. Using the coordinate transformation

$$\mathbf{q}(t) = \mathbf{U}\mathbf{x}(t) \tag{1.2}$$

and assuming low modal damping in system (1.1) yields

$$\ddot{\mathbf{x}}(t) + \text{diag}(2\zeta\omega_j)\dot{\mathbf{x}}(t) + \text{diag}(\omega_j^2)\mathbf{x}(t) = \mathbf{U}^T\mathbf{F}(t) \tag{1.3}$$

where $\mathbf{U}$ is the $n \times n$ modal matrix normalized with respect to the mass matrix, i.e., $\mathbf{U^T M U} = \mathbf{I}$. The variables ω_j and ζ are the jth structural natural frequency and assumed modal damping ratio.

Taking the Laplace transform of (1.3) and substituting into (1.2) yields the input/output transfer function in modal coordinates

$$q_i(s) = \sum_{j=1}^{n}\sum_{k=1}^{n} \frac{u_{ij}u_{kj}}{s^2 + 2\zeta\omega_j s + \omega_j^2} F_k(s) \tag{1.4}$$

where $u_{i,j}$ and $u_{k,j}$ represent the i,j or k,j (row, column) component of $\mathbf{U}$.

Equation (1.4) represents the position response measured at physical coordinate location i due to force inputs at multiple physical coordinate locations $k = 1 \ldots n$. For example, if the flexible structure is simplified as a lumped parameter mass-spring model, (1.4) represents a transfer function for the output measured at mass i due to an input force on mass k. For the collocated SISO systems under investigation, the single force input is at the same location as the measured output ($k = i$). This results in the following system transfer function in modal summation form

$$G_i(s) = \frac{q_i(s)}{F_i(s)} = \sum_{j=1}^{n} \frac{u_{ij}^2}{s^2 + 2\zeta\omega_j s + \omega_j^2} \tag{1.5}$$

The magnitude of the u_{ij} component represents the contribution of the jth structural mode to the overall response seen at coordinate location i.

Figure 1.3 shows the general system in Fig. 1.1 with a linear controller and plant dynamics represented in transfer function form.

The open-loop transfer function for the linear part of this closed-loop system including a PID controller is

$$\begin{aligned} G(s) &= K(s)G_p(s) \\ &= \left(K_p + K_d s + \frac{K_I}{s}\right) \sum_{j=1}^{n} \frac{a_j}{s^2 + 2\zeta\omega_j s + \omega_j^2} \end{aligned} \tag{1.6}$$

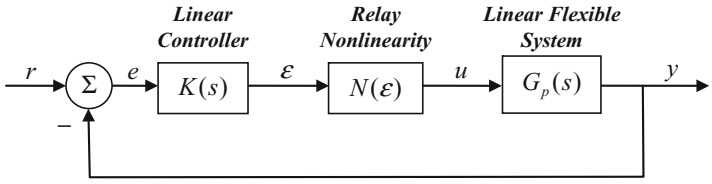

Fig. 1.3 Closed-loop system model

where $a_j = (u_{ij})^2$ from (1.5). The parameters K_p, K_I, and K_d represent the proportional, integral, and derivative gains of the PID controller.

Note that the structure of (1.6) allows the state–space to be formulated into a block diagonal matrix form by inspection. This block diagonal form allows the solution of the closed loop system in Fig. 1.1 to be obtained in closed form, thus eliminating the need for use of numerical techniques in matrix inversion and evaluating of the matrix exponential.

For a Proportional (P) or Proportional-Derivative (PD) Controller

$$\mathbf{A} = \begin{bmatrix} A_0 & & & \\ & A_1 & & \\ & & \ddots & \\ & & & A_n \end{bmatrix}, \quad \mathbf{B} = \begin{bmatrix} B_0 \\ B_1 \\ \vdots \\ B_n \end{bmatrix}, \quad \mathbf{C} = [C_0 \quad C_1 \quad \cdots \quad C_n] \tag{1.7}$$

For Rigid-Body Modes

$$A_0 = \begin{bmatrix} 0 & 1 \\ 0 & 0 \end{bmatrix}, \quad B_0 = \begin{bmatrix} 0 \\ u_{i0} \end{bmatrix}, \quad C_0 = [K_p u_{i0} \quad K_d u_{i0}] \tag{1.8}$$

For Flexible Modes

$$A_i = \begin{bmatrix} 0 & 1 \\ -\omega_j^2 & -2\zeta_j \omega_j \end{bmatrix}, \quad B_i = \begin{bmatrix} 0 \\ u_{ij} \end{bmatrix}, \quad C_i = [K_p u_{ij} \quad K_d u_{ij}] \tag{1.9}$$

where K_p and K_d are position and velocity feedback gains. For a proportional-integral (PI) or PID-type controller, the above equations are augmented with an additional state to account for the integral term.

If the controller is nonlinear, the K_p and K_d gains in output vector $\mathbf{C}$ in (1.7) are set to unity. Any control gains would be applied to the physical coordinates $\mathbf{q}$ given by (1.2) in a nonlinear combination given by $\sigma(x)$ in (1.10). For a linear controller, $\sigma(x) = \mathbf{C}x$.

1.3 Computation of Periodic Solutions

Frequency domain methods such as the DFM (Gelb and Vander Velde 1968) and locus of a perturbed relay system (LPRS) (Boiko 2009) can provide estimates of limit cycle frequency and amplitude, but not periodic fixed point locations (or initial conditions) in modal state space. The limit cycle fixed point locations are necessary for defining the Poincare mapping region of interest. In order to find the fixed points, it is necessary to cast the problem in the state–space form shown in Fig. 1.4 and (1.10). This form assumes $r = 0$ in Fig. 1.1, which is true for the limit cycle analysis considered here. Thus, the new system output y is now the negative of controller output ε shown in Fig. 1.1.

$$\begin{aligned} \dot{x} &= \mathbf{A}x + \mathbf{B}u(y) \\ y &= \sigma(x) \end{aligned} \tag{1.10}$$

$$u(y) = \left\{ \begin{array}{ll} -M & \text{if } y(t) \geq +(\delta + \Delta) \ldots \\ & \quad \text{or } y(t) \geq +(\delta - \Delta) \text{ and } u(t^-) = -M \\ +M & \text{if } y(t) \leq -(\delta + \Delta) \ldots \\ & \quad \text{or } y(t) \leq -(\delta - \Delta) \text{ and } u(t^-) = +M \\ 0 & \text{otherwise} \end{array} \right\}$$

The system input $u(y)$ represents a relay nonlinearity with dead-zone δ, hysteresis Δ, and magnitude M, based on the feedback signal $y(t)$. The matrices $\mathbf{A}$ and $\mathbf{B}$ are defined in (1.7). The output $y(t)$ is a general function of the state variables $x(t)$.

In order to determine the limit cycle frequency using the above state–space equations, it is necessary to calculate the time at which the relay switches under limit cycling conditions. It is assumed that the limit cycle is symmetric, with only two switches and two resets per cycle. These are the characteristics of unimodal periodic motion, and the waveform and input/output relations are shown in Fig. 1.5. The periodic motion is unimodal in the sense that the number and sequence of relay switches and resets per period does not change.

In order for the symmetric unimodal limit cycle in Fig. 1.5 to exist in the system given in (1.10), the following must hold.

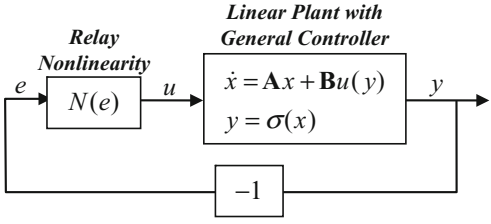

Fig. 1.4 Rearranged closed-loop system model

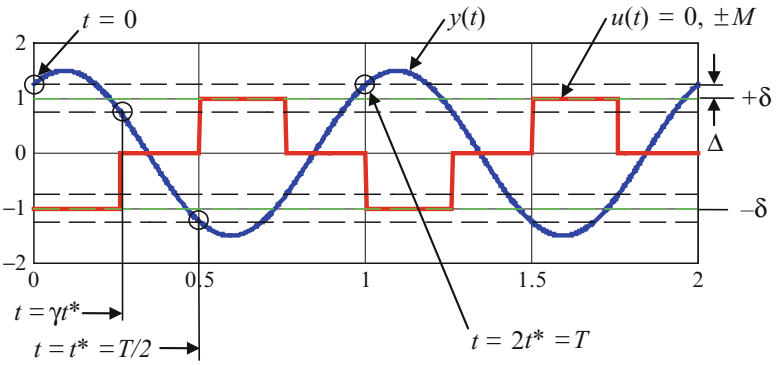

Fig. 1.5 Symmetric unimodal limit cycle waveform in relay feedback system

$$\begin{aligned} y(t) &= y(t+T) && \text{the motion is periodic with period } T \\ y(t) &= -y(t+T/2) && \text{the motion has odd symmetry} \end{aligned} \tag{1.11}$$

Equation (1.11) provides constraints on the system motion for establishing the periodic conditions required for the limit cycle to exist. Using the relations in (1.11), the initial conditions of the state must satisfy

$$x(t^*) = -x(0) \tag{1.12}$$

where t^* is the limit cycle half-period.

In the general case there may be many relay switches occurring during the limit cycle period, and the waveform need not be symmetric. Since the system is piecewise linear with constant input between relay switches, the state equation and its solution between switches are given by

$$\dot{x} = \mathbf{A}x + \mathbf{B}d_i \tag{1.13}$$

$$x(t) = \mathrm{e}^{\mathbf{A}(t-\gamma_{i-1}T)}x(\gamma_{i-1}T) + \int_0^{t-\gamma_{i-1}T} e^{\mathbf{A}\tau}d\tau\mathbf{B}d_i \tag{1.14}$$

$i = 1, 2, \ldots, s, s =$ number of switches while $0 < t \leq T, \gamma_0 = 0, \gamma_s = 1$
$d_i =$ relay magnitude for $\gamma_{i-1}T < t \leq \gamma_i T$

where $\gamma_i T$ is the time at relay switch i as a fraction of limit cycle period T. The γ_i parameter for each successive switching instance obeys the following constraint

$$0 < \gamma_1 < \gamma_2 < \cdots < \gamma_{s-2} < \gamma_{s-1} < 1 \tag{1.15}$$

For the assumed symmetric limit cycle waveform shown in Fig. 1.5, it is only necessary to consider the waveform during the first half-period t^* of the limit cycle. And for the assumed relay with dead-zone and hysteresis, the number of switches during this half-period is two ($s = 2$). One switch off at γt^* and one switch to $+M$ at t^*. Substituting $s = 2$ and $T = t^*$ into (1.14) yields

$$x(t) = \mathrm{e}^{\mathbf{A}(t-\gamma_{i-1}t^*)}x(\gamma_{i-1}t^*) + \int_0^{t-\gamma_{i-1}t^*} e^{\mathbf{A}\tau}d\tau\mathbf{B}d_i \tag{1.16}$$

$$i = 1, 2,\ \gamma_0 = 0, \gamma_1 = \gamma, \gamma_2 = 1$$
$$d_i = \text{relay magnitude for } \gamma_{i-1}t^* < t \le \gamma_i t^*$$

Noting in Fig. 1.5 that relay magnitude $d_1 = -\mathrm{M}$ and $d_2 = 0$, (1.13) yields the following state dynamics between switches.

$$\begin{aligned} \dot{x} &= \mathbf{A}x - \mathbf{B}M \qquad \text{for} \qquad 0 < t \le \gamma t^* \\ \dot{x} &= \mathbf{A}x \qquad\qquad\ \text{for} \qquad \gamma t^* < t \le t^* \end{aligned} \tag{1.17}$$

At relay reset time $t = \gamma t^*$ the output $y(t)$ is crossing the upper dead-zone minus hysteresis boundary $(\delta - \Delta)$ of the relay with negative slope $(\dot{y}(t)<0)$. At relay switching time $t = t^*$, the output $y(t)$ is crossing the lower dead-zone plus hysteresis boundary$(-(\delta + \Delta))$ of the relay with negative slope. The state solution (1.16) at these instants in time and the symmetry constraint (1.12) can be used to determine the initial conditions that result in a limit cycle

$$\begin{aligned} x(\gamma t^*) &= \mathrm{e}^{\mathbf{A}\gamma t^*}x(0) + \int_0^{\gamma t^*} e^{\mathbf{A}\tau}d\tau\mathbf{B}(-M) \\ x(t^*) &= \mathrm{e}^{\mathbf{A}(t^*-\gamma t^*)}x(\gamma t^*) = -x(0) \end{aligned} \tag{1.18}$$

$$\text{yielding } x(0) = \left(\mathrm{e}^{\mathbf{A}t^*} + \mathbf{I}\right)^{-1} \int_{t^*-\gamma t^*}^{t^*} e^{\mathbf{A}\tau}d\tau\mathbf{B}M \tag{1.19}$$

Also, referring to Fig. 1.5, at $t = 0$ and the subsequent switching instant, the relay input crosses the hysteresis bands as follows:

$$\begin{aligned} y(0) &= \sigma(x(0)) = +(\delta + \Delta) \\ y(\gamma t^*) &= \sigma(x(\gamma t^*)) = +(\delta - \Delta) \end{aligned} \tag{1.20}$$

Solutions of γ, and t^* which satisfy (1.20) are obtained numerically, yielding limit cycle frequencies of $\omega^* = \pi/t^*$. Note that an initial guess is required for the

parameter γ. For the assumed unimodal symmetric limit cycle waveform, this parameter obeys the following constraint

$$0 < \gamma < 1 \tag{1.21}$$

The following additional waveform criterion must be satisfied in order for the solution to be a limit cycle (see Fig. 1.5).

To ensure proper velocity direction at switches

$$(i)\,\dot{y}(0) > 0, \qquad (ii)\,\dot{y}(\gamma t^*) < 0 \tag{1.22}$$

To ensure proper waveform between switches

$$\begin{aligned} &(i) \quad y(t) > +(\delta - \Delta), \qquad 0 < t < \gamma t^* \\ &(ii) + (\delta + \Delta) > y(t) > -(\delta + \Delta), \qquad \gamma t^* < t < t^* \end{aligned} \tag{1.23}$$

Local stability of the limit cycle is satisfied using the Jacobian of the Poincaré map given by

$$\begin{aligned} \mathbf{W} = &\left[\Phi_2 - v_2\left(\frac{\sigma_x{}^{\langle 2\rangle}(x(\gamma t^*), t^*)}{\sigma_t{}^{\langle 2\rangle}(x(\gamma t^*), t^*)}\right)\right] \times \ldots \\ &\left[\Phi_1 - v_1\left(\frac{\sigma_x{}^{\langle 1\rangle}(x^*, \gamma t^*)}{\sigma_t{}^{\langle 1\rangle}(x^*, \gamma t^*)}\right)\right] \end{aligned} \tag{1.24}$$

where

$$\begin{aligned} x^* &= \text{initial condition fixed point on} \\ &\quad \text{switching surface } \sigma(x^*) = +(\delta + \Delta) \\ x(\gamma t^*) &= \text{relay reset fixed point on} \\ &\quad \text{switching surface } \sigma(x(\gamma t^*)) = +(\delta - \Delta) \\ \Phi_1 &= e^{\mathbf{A}\gamma t^*}, \Phi_2 = e^{\mathbf{A}(t^* - \gamma t^*)}, \gamma t^* = \text{relay reset time}, \\ t^* &= \text{limit cycle half - period} \\ v_1 &= \mathbf{A}x(\gamma t^*) - \mathbf{B}M \text{ state velocity just before} \\ &\quad \text{reset from } -M \text{ to } 0 \text{ at } x(\gamma t^{*-}) \\ v_2 &= \mathbf{A}(-x^*) \text{ state velocity just before switch} \\ &\quad \text{from } 0 \text{ to } +M \text{ at } x(t^{*-}) \end{aligned}$$

and the partial derivative terms of the output equation $\sigma(x(t))$ with respect to x and t are evaluated using the state dynamics between switching instances (1.16) and (1.17) (refer to Borre (2011) for details). This approach is an extension of the work

by Astrom (1995), where the method presented here includes a nonlinear switching surface and relay with dead-zone and hysteresis. The limit cycles are locally stable if the eigenvalues of **W** in (1.24) lie within the unit circle.

1.4 Region of Attraction Mapping

1.4.1 Simple Cell Mapping

The region of attraction for periodic solutions of a system can be found by mapping methods. One such method, known as SCM, was developed by Hsu (1987). Each point mapping consists of integrating the system equations of motion over a predetermined fixed integration time period T.

The region of interest in an n dimensional state–space is discretized into N cells along each dimension for a total of N^n cells. The center point of each cell serves as the starting location (initial conditions) for the mapping procedure. The center point of the destination cell that the system trajectory ends up in after one integration period is the mapping of the originating cell. For example, referring to Fig. 1.6, cell Z_1 maps to Z_{15}, Z_{15} maps to Z_8, and Z_8 maps back to Z_{15}.

For a periodic solution to exist, trajectories from the originating cell eventually return to this cell after k integration periods of duration T. This is called a "P–K" periodic solution. Figure 1.6 shows a P-2 periodic solution, initiating from cell Z_{15} and returning to cell Z_{15}, after two integration periods. Note that the period of

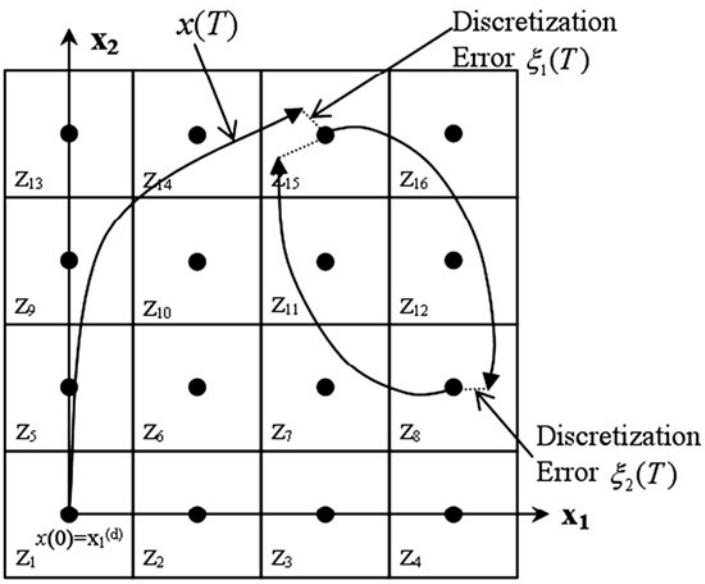

Fig. 1.6 System trajectory for integration period T in state–space coordinates

integration T is typically not the same as the limit cycle period. An efficient sorting algorithm developed by Hsu and Guttalu (1980) sorts and characterizes each individual cell with what Hsu defines in Hsu (1987) as a P Number and Group Number, which differentiates the state–space into ROA for each different P–K solution that exists.

The cell mapping process is essentially defining the mapping of *every* initial state that lies within the originating cell boundary to *every* final state that lies within the boundary of the destination cell. Thus there is a discretization error that occurs when the cell space discretization is relatively coarse. To improve the mapping results, the discretization is refined. As noted above, the cell space consists of N^n cells, so the cell space and thus computer memory requirements grow exponentially with refinement. While this method is attractive in its simplicity, the computer memory requirements make this method difficult to apply for systems with more than 2 degrees-of-freedom (four states).

1.4.2 Switching Surface Poincare Cell Map (SSPCM)

The new method presented here extends two existing methods in a novel way, allowing the study of limit cycle ROA for systems under relay feedback control with linear plants that include structural flexibility. First, the time-based state–space method for limit cycle determination described in the previous section, which is typically applied to local stability analysis of process plant-type applications with a single limit cycle (Astrom 1995), is now applied to structural vibration problems with multiple flexible modes. Once the limit cycle frequencies and periodic fixed points are known, the region of interest can be mapped to determine the ROA for each limit cycle. Since the periodic fixed points lie on the relay switching surface, the switching surface is selected as the Poincare mapping surface. Second, the new method applies the Poincare-like SCM method described in Levitas (Levitas et al. 1994) to the relay switching surface, in order to significantly reduce the memory requirements described above for SCM (Hsu 1987).

The following Figure 1.7 shows how switching instances of a relay in the same direction, can be used to define the Poincare mapping surface. Every time the relay

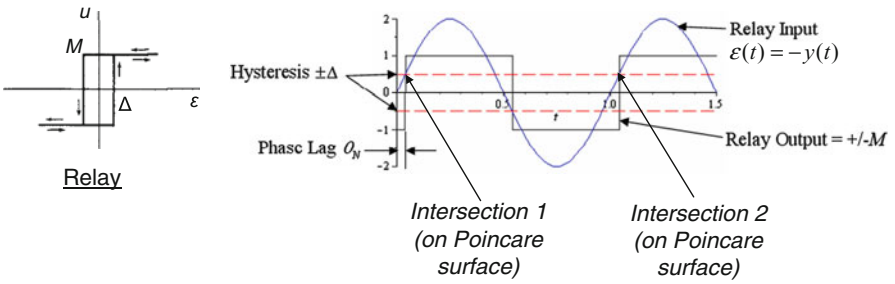

Fig. 1.7 Mapping surface defined as relay input causing switch in positive direction

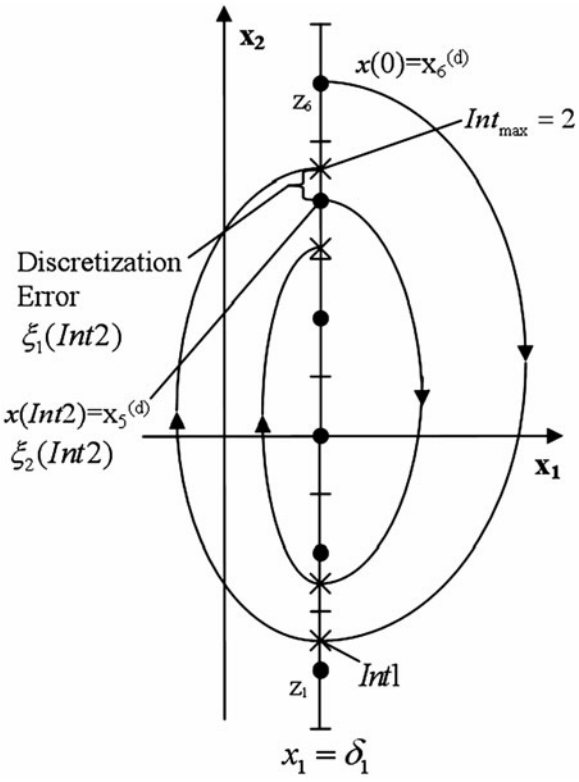

Fig. 1.8 Two-state system trajectory between switching surface intersections

input reaches the positive hysteresis bound with positive slope causing a switch, the state at this instance is noted (mapped) as an intersection with the Relay Switching Surface. Note that the map can be produced by periodic switches on any switching surface, as long as the relay input and output are consistent at each switch.

Figure 1.8 shows an example of the Poincare surface for a 2D system that would be discretized into a cell space. Trajectories are integrated forward from each cell center for a prescribed number of surface intersections ($\text{Int}_{\max}$), defining the final location or "map" of each cell (Levitas et al. 1994). In Fig. 1.8, the trajectory started at the center of cell Z_6 is integrated until two intersections with the Poincare surface are encountered ($\text{Int}_{\max} = 2$). The cell at this location (Z_5) is the map of the originating cell. The center of this cell then becomes the starting point for integration until the specified intersections is reached. This is repeated until a previously processed cell is reached (Z_5 in this case).

As stated above, the surface selected to act as the Poincare surface for the new method is the surface that defines the relay switching in one direction. Using the Levitas method allows the reduction of the cell map dimensions from $\mathbf{R}^N$ to $\mathbf{R}^{(N-1)}$, where N is the number of states of the system. Since the number of cells in the cell space grows exponentially, this results in a significant reduction in total number of cells for larger order systems.

1.4.3 Integration Stopping Criterion

An extension of Levitas' Method is implemented in the new method. One limitation to Levitas' Method is that the total number of intersections with the switching surface is somewhat arbitrarily selected beforehand. Convergence of the map is determined by performing successive mappings of the entire cell space, and noting changes in the map. When there is acceptable agreement, the map has converged. This is difficult to determine, especially for higher order systems.

Also, each cell is mapped for the same number of intersections, regardless of how close it is to convergence. Thus, initial conditions close to periodic fixed points are integrated for the same number of intersections as initial conditions far away from the fixed point. This results in unnecessary integration time for points close to the fixed points. The proposed method employs a convergence criterion that can be specified ahead of time, which will allow only the minimum number of surface intersections necessary for convergence.

Note that for a periodic limit cycle to exist, the following mapping holds for consecutive relay switches.

$$x((n+1)T) = G(x(nT)) \quad n = 0, 1, 2... \tag{1.25}$$

In the general case, the mapping $G(x(nT))$ is not known; however, for the relay feedback case at hand, it is determined numerically as the system is integrated from one relay switch to the next. Since the system trajectory is mapped at each switch, convergence to a periodic solution can be determined by the distance between each consecutive intersection with the switching surface in the proper direction as shown in Fig. 1.9.

The error convergence criterion shown in (1.26) is checked at each relay switch, and a determination is made whether to keep integrating for one more switch, or to stop and set the period for the current cell. This period is defined as the switching time for the last switch.

$$x_{\text{error}} = \frac{\|x(t_{n+1}) - x(t_n)\|}{\|x(t_n)\|} \leq \kappa \quad n = 0, 1, 2... \tag{1.26}$$

$x(t_n)$ = state variable coordinates on the switching plane
n = number of relay switching instance in proper direction
$n = 0$ for initial condition at center of originating cell

Since the final time between consecutive switches is known for the current converged mapping instance, this time can be compared with the exact limit cycle periods determined using the state–space method. Thus, the originating cell and the final mapped cell are both determined to be part of the region of attraction for this particular limit cycle.

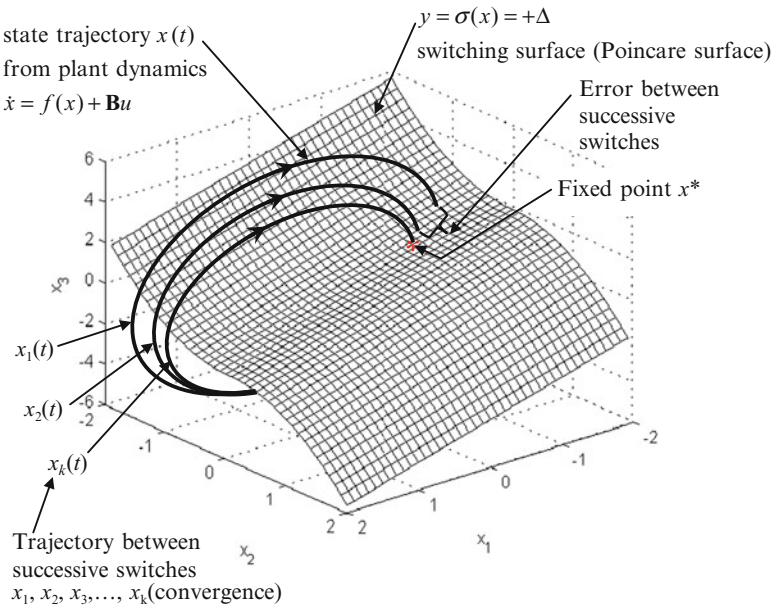

Fig. 1.9 Converging trajectory between switching surface intersections

Three other error criteria are checked at each switching surface intersection, and indicate that the trajectory is not converging to a periodic fixed point. These are the maximum error between successive switches (divergence), the maximum time between successive switches, and the maximum number of total switches. If any of these criteria are violated, the integration routine is stopped, and the current cell maps to the sink cell. These criteria are designed to reduce overall integration time, and are problem dependent. A simulation starting from a point that maps to the sink cell can reveal if these criteria need to be relaxed or tightened.

Once the switching surface has been mapped, any trajectory that lands on the switching surface has the limit cycle properties of the cell that encloses that point. This allows other initial conditions to be evaluated that do not lie on the switching surface, simply by noting the first intersection with the switching surface in the proper direction. However, the above error convergence criterion pertains to trajectories started from the center point of each cell. There is a discretization error introduced when intersecting the switching surface at locations other than the cell centers. This error can be reduced by increasing the cell density on the switching surface.

An alternative mapping that retains the above error convergence criterion can be produced, using the proposed method with initial conditions that are not on the switching plane. However, the cell space of this map no longer has the reduced dimension $\mathbf{R}^{(N-1)}$, but has the full state–space dimension $\mathbf{R}^N$. Note that the exponential increase in the total number of cells of the alternate map may still be much greater than that of the refined switching surface map, making it less attractive than the refined switching surface map. For example, the total number of cells on a